Numerical Validation of the Efficiency of Dual-Frequency Radiofrequency Ablation

A. Candeo[*1], and F. Dughiero[1]

[1]Department Electrical Engineering, University of Padova, Padova, Italy

*Corresponding author: via Gradenigo, 6/a – 35131 Padova (alessandro.candeo@unipd.it)

Abstract: *Radiofrequency ablation (RFA) represents a valid alternative for treating liver metastases in medically complicated patients. Conventional devices currently operate at 500 kHz, due to good conducting properties of tissues. However, the use of lower frequencies (i.e., 20 kHz) has been recently reported to enhance the treatment effectiveness, due to a more pronounced difference in electrical properties between tumor and liver tissue. This results in focusing higher power densities in the tumor area, rather than in surrounding tissue, thus producing higher heating rates. The effect of different frequency values was investigated by means of numerical simulation. A specific model was developed and tested under specific operating conditions. Both single and dual-frequency modes were considered, by using a constant or variable input feed. Dual-frequency approach appears to successfully combine the advantages of each single frequency alone, thus providing overall higher temperatures together with lower local overheating.*

Keywords: Radiofrequency Ablation (RFA), Dual-Frequency, Blood Perfusion, Temperature Control, Tail-Effect

1. Introduction

Clinical hyperthermia consists in the generation of a higher temperature at a tumor-involved region of the body. One of the crucial evidences which have allowed the development of clinical hyperthermia as cancer treatment, relates with the different sensitivity that healthy and impaired tissues exhibit when they are heated. Among the different approaches that can be used, percutaneous radiofrequency ablation (RFA) is one of the most widespread, due to its minimal invasiveness, standard clinical application, and successful outcome. This technique exploits the electrical energy radiated from a needle electrode to create a coagulative necrosis within surrounding tissues, through the application of alternating RF stimuli. Usually, the applied frequency range is between 200 and 500 kHz. Various improvements have been tested through years (e.g., internally water-cooled tips, multi-prong electrodes, and cluster applicators), thus making it possible to treat lesions up to 5 cm in diameter [1]. However, since the value of the electrical conductivity of healthy versus impaired tissue in the conventional frequency range is quite similar, a poor outcome is obtained in terms of heating selectiveness.

Recent studies have reported a much higher difference in conductivity at lower frequencies (e.g., 20 kHz), which would produce a substantial change in the specific absorption rate (SAR) deposition and a preferential heating of the tumor mass [2]. This effect is particularly pronounced when the active tip of the electrode is positioned across the tumor boundary, being partly in contact with surrounding normal tissue.

In clinical routine, RFA is mainly used in the treatment of liver metastases from colorectal cancers and lung neoplasms [3, 4], as well as kidney and thoracic diseases [5].

2. Use of COMSOL Multiphysics

2.1. Geometry Description

A 2D axis-symmetric model of the treatment zone was developed (Fig. 1), consisting of two concentric subdomains: the inner one (diameter: 20 mm) represents the tumor nodule and is surrounded by an outer region (diameter: 100 mm), representing normal liver tissue; a 1.5 mm (17 gauge) thick catheter region, including a 30 mm internally-cooled active tip in the distal part, was inserted in the middle of the model, thus completely covering the tumor mass, as well as 10 mm of normal liver tissue. This is a common layout used in clinical application, since it allows the heating of a marginal extra-tumor area of possibly-mutagen tissue, thus improving overall recovery rate and reducing recurrences [6].
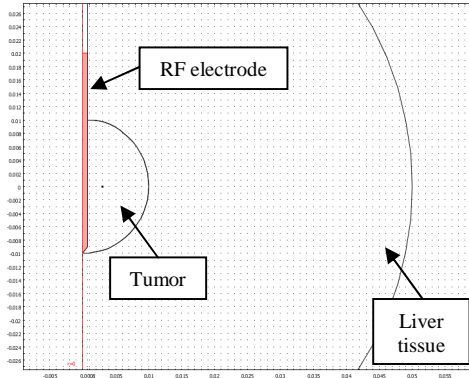
Figure 1. Schematics of the model geometry

2.2. Governing Equations and Application Modes

A coupled dielectro-thermal transient simulation was performed, by using the Meridional Electric Currents and the Bioheat Equation application modes. The former computes the electric field intensity $E = -\nabla V$ and current density $J = \sigma E$ by solving the following Laplace's equation in the electric potential V:

$$-\nabla \cdot (\sigma + j\omega\varepsilon_0\varepsilon)\nabla V = 0,\qquad(1)$$

where σ is the electric conductivity of tissues (S/m), ε is the relative permittivity, ω is the angular frequency (rad/s), and ε_0 is the vacuum dielectric constant (8.85e-12 F/m).

The latter evaluates the evolution of the temperature T originating from the thermal source $J \cdot E$, by solving the so-called Bio-Heat Transfer Equation from Pennes [7]:

$$\rho c \frac{\partial T}{\partial t} + \nabla \cdot (-k\nabla T) = \rho_b c_b \omega_b (T_b - T) + J \cdot E, \quad(2)$$

where ρ is the mass density of tissues (kg/m³), k their thermal conductivity (W/m/°C), and c their specific heat capacity (J/kg/°C); the subscript b indicates the quantities referred to the blood, in particular the blood perfusion coefficient ω_b (s⁻¹), which accounts for thermal exchange phenomena occurring in the capillary bed at the equilibrium T_b (37 °C).

2.3. Boundary Conditions and Material Properties

The active tip of the RF electrode was constrained to have a given electric potential V_0 (in order to model the feeding source), as well as a given temperature value T_0 (15 °C, in order to model the internal coolant); at the tissue outmost boundary the ground condition was used, together with an imposed value to account for basal body temperature (37 °C) away from the treatment area. The initial temperature for the thermal transient analysis was 37 °C.

In order to account for the change in conduction properties of tissues during heating, a temperature-dependence for both electrical and thermal conductivities was assumed, obeying to the following expressions:

$$\sigma(T) = \sigma(T_b)\big(1 + \alpha_\sigma(T - T_b)\big)$$
$$k(T) = k(T_b) + \alpha_k(T - T_b)\qquad(3)$$

where the temperature coefficients α_σ and α_k were set to 0.015 (°C⁻¹) and 0.00116 (W/m/°C²), respectively; Gabriel's data was used for frequency-dependent values of tissue dielectric properties [8]. A list of the values used in the simulations is reported in Tab. 1.

Table 1: Material properties used in the simulations.

Property	Liver	Tumor
Relative permittivity ε_r (20 kHz)	18516	
Relative permittivity ε_r (500 kHz)	2770	
Dielectric conductivity σ (20 kHz)	0.17 (S/m)	0.31 (S/m)
Dielectric conductivity σ (500 kHz)	0.36 (S/m)	0.45 (S/m)
Thermal conductivity k	0.512 (W/m/°C)	0.570 (W/m/°C)
Blood perfusion coefficient ω_b	16.670e-3 (s⁻¹)	0.416e-3 (s⁻¹)

2.4. Type of analysis

Two different types of analyses were carried out in the course of a 600-second transient simulation, defined by a constant or variable feeding input approach. All the results have been compared in terms of SAR and temperature color maps of the domain, temperature evolution plots related to critical treatment areas, and spatial temperature distribution along different paths.

With the constant feed, the effect of different operation frequencies was investigated, by comparing the effects produced by a given amount of power dissipated within tissues (e.g., 40 W). In this case, the input voltage was manually adjusted *a posteriori*, in order to obtain comparable losses in the computational domain.

With the variable feed, the behavior of a real medical ablation device can be simulated, which automatically adjusts the applied voltage *in line*, in order to keep the maximum temperature value below the vaporization limit (100 °C); in fact, heating above this value would result in abrupt decrease of tissue conductivity, thus causing the heating to be ineffective and eventually leading to charring.

In this case, a MATLAB connection was used to implement the feedback loop driving the input voltage, based on a classic proportional rule:

$$V = V_0 + K_p(T_{max} - T), \qquad (4)$$

where the gain K_p was manually tuned in order to obtain the lowest oscillation; V and V_0 represent current and initial voltage, while T and T_{max} current and threshold temperature, respectively. The problem was then split into a sequence of steps, at the end of which a separate solution was evaluated and the controlled variable updated accordingly; at the end of the process, after a number of loops dependent on the chosen time step (ranging between 1 and 15 s) the final solution was obtained. A schematic view of the solution script is reported in Fig. 2.

The effect of the operation frequency was investigated by comparing and validating lower (i.e., 20 kHz) and conventional (i.e., 500 kHz) frequencies; moreover, a brand-new dual-frequency approach was pursued, which accounted for the simultaneous effect of different frequencies; this was accomplished by superimposing the power density distributions originating from two separate harmonic simulations into the thermal computation. For this purpose, two concurrent application modes were used and fed each with 50% of the required power, thus producing comparable results.
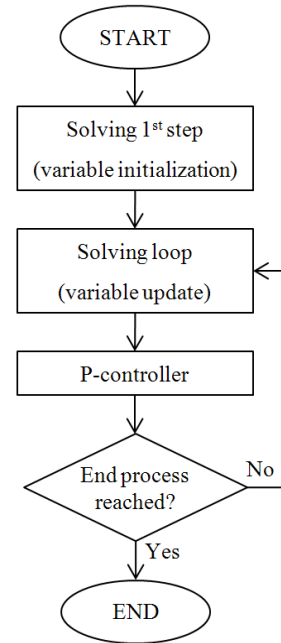

Figure 2. Flowchart of the implemented MATLAB routine.

3. Results

In this section a description of the main findings obtained from the considered case studies will be given.

3.1. Constant Feed

In order to compare the effects of different frequencies when a constant voltage feed is used, each model has been tuned so as to obtain a similar value for power losses within the computational domain. According to preceding experience [9] and clinical reference [5], this value was chosen to be 40 W, a relatively low power level, which is typically used in conjunction with treatment times ranging between 7 and 12 minutes. More details about the simulation parameters considered for each operation mode is reported in Tab. 2.

Table 2: Constant feed data summary.

Operation mode	Applied voltage	Domain losses
20 kHz	77 (V)	40.1 (W)
500 kHz	57 (V)	40.0 (W)
dual-frequency	67 (V)	39.5 (W)

The SAR deposition exhibits a different pattern depending on the frequency of sources. In particular, lower frequencies (20 kHz) appear to preferentially focus the energy inside the tumor, thus producing a more selective heating of the mass and a better coverage of the marginal area (Fig. 3).
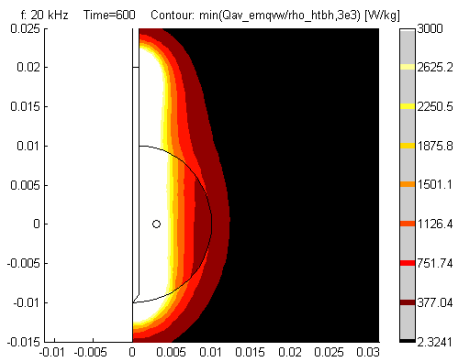

Figure 3. SAR deposition (W/kg) with 20 kHz source.
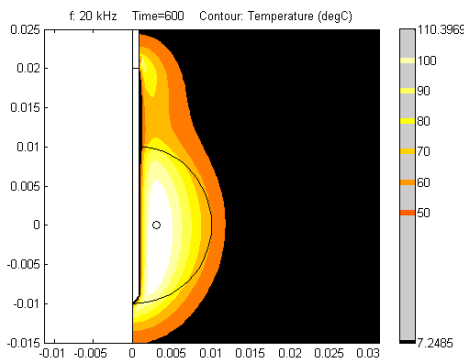
Figure 4. T distribution (°C) with 20 kHz source.

Conventional frequencies (500 kHz) exhibit a lower penetration into tissues as well as a more uniform deposition between tumor and normal tissue (Fig. 5), thus producing a less selective heating of the mass.
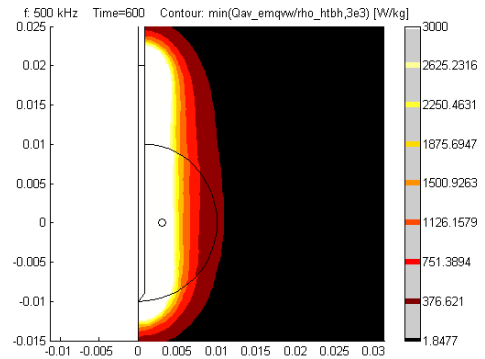

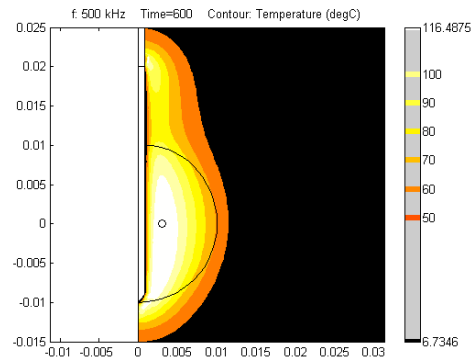**Figure 5.** SAR deposition (W/kg) with 500 kHz source.

Figure 6. T distribution (°C) with 500 kHz source.

At a first glance however, the resulting thermal maps in the tumor at the end of the treatment are quite similar (Figg. 4, 6). Major differences can be found at the interface with surrounding healthy tissue, where a slight overheating is registered in the proximity of the electrode (the so-called "tail-effect"). Moreover, the resulting thermal lesion (i.e., the area of tissue enclosed by the 50 °C isothermal line) is comparable both in shape and size between the two single frequencies. This fact is confirmed by inspection of temperature distribution plots and temperature evolution in the target area (Fig. 9): a

comparable heating of the tumor is achieved, with each single frequency mode, in the longitudinal (z-axis) section, while a noticeable reduction in temperature (approx 8 °C) is obtained, with 20 kHz, in the zone of normal tissue close to the electrode.

When dual-frequency operates (Figg. 7, 8), a more effective heating of the tumor mass is experienced: in fact, higher temperature profiles are found in the cross-section plot along a path facing the electrode. Furthermore, compared to 500 kHz, a reduced tail-effect is obtained (see dashed line in Fig. 9).
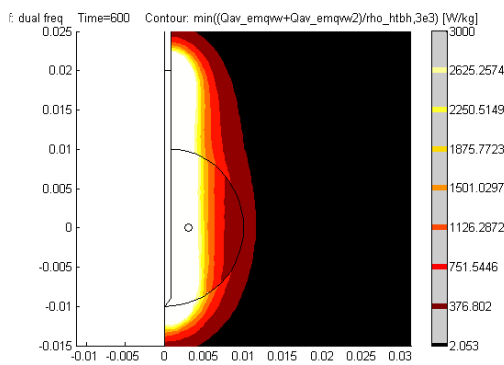

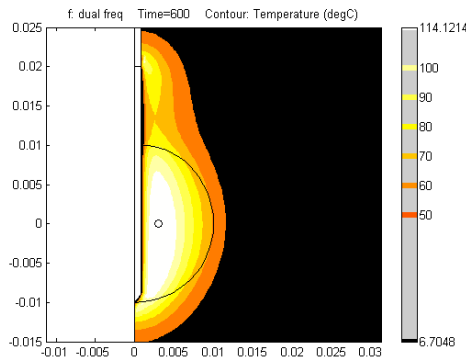**Figure 7.** SAR deposition (W/kg) with dual-frequency mode.

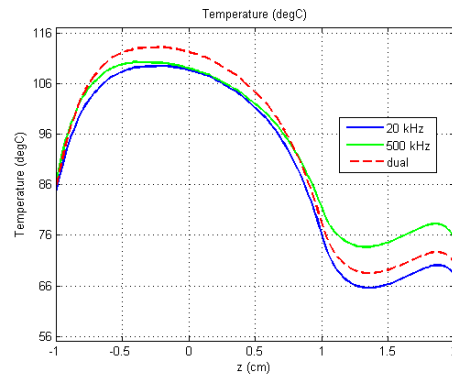**Figure 8.** T distribution (°C) with dual-frequency mode.

Figure 9. T distribution (°C) along a line facing the electrode for different operation modes. The tumor is centered at z=0 mm.

3.2. Variable Feed (P controller)

In the case of modeling of the control algorithm employed in medical RF generators through a P (Proportional) controller, the analysis can be performed regardless to the actual value of domain losses, as the controller takes on the burden of automatically adjusting the applied voltage, based on the control rule. For this reason, care must be taken in choosing the starting voltage only: in fact, an higher value could lead to temperature oscillation, while a lower value would extend heat-up times. Resulting steady-state voltage values and overall domain losses are reported in Tab. 3.

In general, we can observe an overall increase in power losses values, which are obtained with lower feeding voltages.

Table 3: Variable feed data summary.

Operation mode	Steady state voltage	Average losses
20 kHz	71 (V)	43.6 (W)
500 kHz	51 (V)	42.1 (W)
dual-frequency	62 (V)	44.4 (W)

Many similarities with previous case are found; in particular, SAR and temperature maps don't

show much of a difference, while temperature profiles exhibit slightly different trends. In fact, comparable heating of the mass, together with lower tail-effect is experienced at 20 kHz (Fig. 10), while shorter heat-up phase is required with 500 kHz (Fig. 11); interestingly, dual-frequency mode produces a sort of combined effect, reducing normal tissue overheating while providing the same heating of the tumor mass (see dashed line in Figg. 10, 11). Furthermore, the heating evolution curve of the tumor core is located in between 20 and 500 kHz, thus causing a faster and progressive heating (Fig. 12).
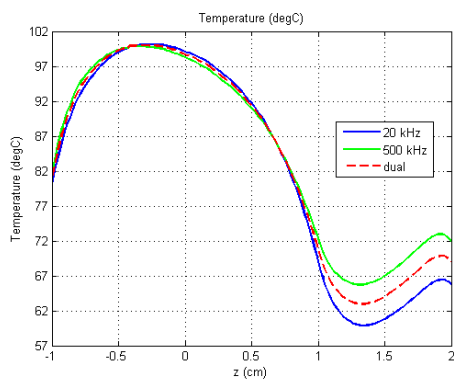

Figure 10. T distribution (°C) along a line facing the electrode for different operation modes. The tumor is centered at z=0 mm.
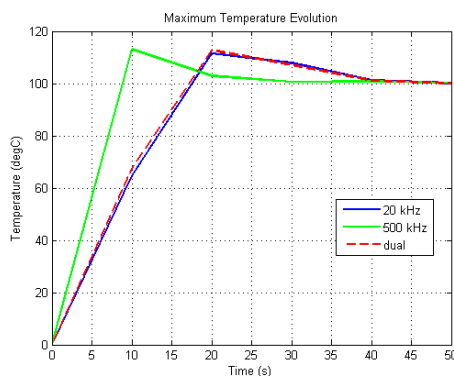

Figure 11. Evolution of the maximum temperature (°C) for different operation modes.
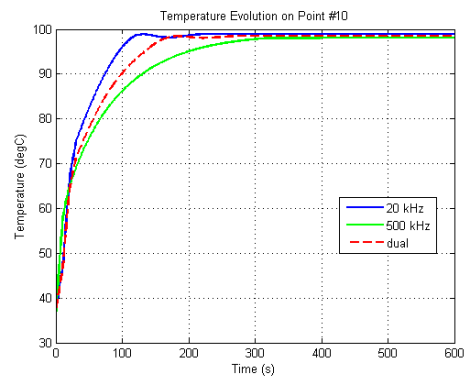

Figure 12. T evolution (°C) in the tumor core for different operation modes. The point has coordinates (r,z)=(3,0) mm.

4. Discussion

The results highlighted in the previous section may lead to a bunch of considerations. First of all, in a constant voltage/power setup, the two considered frequencies don't behave much differently in terms of heating of the tumor, which results to be comparable, both in the peak temperature evolution and in its radial distribution. Only a more pronounced tail-effect can be noticed when 500 kHz operates.

In this setting, dual-frequency mode results in slightly higher peak temperatures and radial distributions, thus more effectively heating the mass and reducing tissue overheating next to the active RF electrode.

When a power control rule is employed, 500 kHz are reported to heat the tissues faster (especially with regard to peak temperatures) but unselectively, while 20 kHz provide a better targeting of the tumor.

A combined effect results from the application of the dual-frequency mode, which takes advantage of the benefits of each single frequency alone, thus producing a fast increase of both core and peak temperatures, while reducing the tail-effect.

5. Conclusions

Due to the more pronounced differences in dielectric properties between normal and tumor tissues, lower frequencies cause a more selective heating of the target area. Higher frequencies exhibit lower penetration inside the tumor and may result in local overheating. This results in

higher unfocused heating. The dual-frequency approach helps to reduce the power density in the tissue, thus reducing undesired hot spots in marginal areas.

6. References

1. *J. M. Lee, J. K. Han, S. H. Kim, et al, Wet Radio-Frequency Ablation using Multiple Electrodes: Comparative Study of Bipolar Versus Monopolar Modes in the Bovine Liver,* **54**, *408, (2005)*

2. *D. Haemmerich and B. J. Wood, Hepatic Radiofrequency Ablation at Low Frequencies Preferentially Heats Tumour Tissue,* **22**, *563, (2006)*

3. *M. Cariati, G. Giordano, M. Midulla, et al, Radiofrequency Ablation of Pulmonary Lesions,* **112**, *149, (2007)*

4. *H. Hur, Y. T. Ko, B. S. Min, et al, Comparative Study of Resection and Radiofrequency Ablation in the Treatment of Solitary Colorectal Liver Metastases, (2008)*

5. *E. vanSonnenberg, W. McMullen, L. Solbiati and T. Livraghi, Tumor Ablation: Principles and Practice , 542. Springer, (2005)*

6. *E. Berjano, Theoretical Modeling for Radiofrequency Ablation: State-of-the-Art and Challenges for the Future Biomedical engineering online,* **5**, *(2006)*

7. *H. H. Pennes, Analysis of Tissue and Arterial Blood Temperatures in the Resting Human Forearm. 1948 J.Appl.Physiol.,* **85**, *5-34, (1998)*

8. *S. Gabriel, R. W. Lau and C. Gabriel, The Dielectric Properties of Biological Tissues: II. Measurements in the Frequency Range 10 Hz to 20 GHz,* **41**, *2251, (1996)*

9. *V. D'Ambrosio, F. Dughiero and M. Forzan, Numerical Models of RF-Thermal Ablation Treatments The International Journal of Applied Electromagnetics and Mechanics,* **25**, *429, (2007)*

7. Acknowledgements

8. Appendix

In order to implement a power controller based on the actual temperature of tissues, the entire solving procedure has been broken down into singular smaller steps. A control rule has then been defined in between each single solution step, which read the tissue temperature, compared it with the set-point value and, if needed, corrected the power level accordingly. The pseudo-code structure is here introduced.

```
% Initialization step %
%
% Solve problem (init)
   fem.sol=femtime(fem, ...
      'solcomp',{'T','V'}, ...
      'outcomp',{'T','V'}, ...
      'blocksize','auto', ...
      'tlist',[colon(0,1,1*tStep)],
      ...
      'tout','tlist', ...
      'linsolver','pardiso', ...
      'pivotperturb','1e-008', ...
      'itol',1e-006, ...
      'rhob',400);

% Optimization step %
%
% while loop %
   % initialize counter
   % controller gain

   while currt(n-1) <= tEnd
   % establish the control rule
   (n-1) = maxT - maxvec(n-1);
   % Proportional contribution
   Vc = currV(n-1)+Kp*e(n-1);

   % Solve problem (loop)
   fem.sol=femtime(fem, ...
      'init',solvec(n-1).sol, ...
      'solcomp',{'T','V'}, ...
      'outcomp',{'T','V'}, ...
      'blocksize','auto', ...
      'tlist',[colon(currt(n-
1),1,currt(n-1)+tStep)], ...
      'tout','tlist', ...
      'linsolver','pardiso', ...
      'pivotperturb','1e-008', ...
      'itol',1e-006, ...
      'rhob',400);

   % save current structure
   solvec(n)=fem;
   % update counter
   n=n+1;
% end while %
```